LASERS

Numerical simulation of amplification of frequency-modulated radiation in a gas amplifier THL-100 laser system

A.G. Yastremskii, N.G. Ivanov, V.F. Losev

Abstract. **Numerical simulation methods have been used to study the effect of frequency modulation of input laser radiation with a pulse duration of 250 ps on the gain characteristics in a gas XeF (C–A) amplifier of the hybrid THL-100 laser system at a pump energy of 270–400 J. Using the Wigner distribution function, local radiation spectra are calculated at various points of the input laser beam with positive and negative chirps. The effect of the pump energy of the amplifier on the energy, intensity, and duration of the output laser radiation pulses is investigated. It is shown that with an insignificant change in energy, the pulse duration of the output radiation turns out to be longer with a negative chirp of the input radiation.**

1. Introduction

In papers by L.D. Mikheev et al. [1, 2], a hybrid scheme of multi-laser laser systems was proposed using the C(3/2) → A(3/2) transition in the XeF molecule. Using this scheme, the THL-100 hybrid laser system was fabricated at the Institute of High Current Electronics, Siberian Branch of the Russian Academy of Sciences (IHCE SB RAS) together with the Lebedev Physical Institute of the Russian Academy of Sciences (LPI RAS). The system includes a Start-480M Ti : sapphire femtosecond front-end, produced by Avesta-Project, and a photodissociation XeF (C–A) amplifier, developed and executed at the IHCE SB RAS together with the LPI RAS. The complex included a Ti : sapphire master oscillator of femtosecond pulses pumped by a Verdi-8 cw laser at λ = 532 nm, a grating stretcher, a regenerative amplifier and two multipass amplifiers pumped by radiation from repetitively pulsed lasers at λ = 532 nm, and a second harmonic generator based on the first-type KDR crystal with a thickness of 2 mm. In 2013, the radiation with a power of 14 TW [3–5], an energy of 0.7 J and a pulse duration of 50 fs was obtained from the THF-100 facility. After increasing the pump energy of the XeF (C–A) amplifier to 270 J, it was possible to obtain the laser radiation energy E_{out} = 3.2 J [3, 6, 7].

A.G. Yastremskii, N.G. Ivanov Institute of High Current Electronics, Siberian Branch, Russian Academy of Sciences, Akademicheskii prosp. 2/3, 634055 Tomsk, Russia; e-mail: ayastremskii@yandex.ru;
V.F. Losev Institute of High Current Electronics, Siberian Branch, Russian Academy of Sciences, Akademicheskii prosp. 2/3, 634055 Tomsk, Russia; National Research Tomsk Polytechnic University, prosp. Lenina 30, 634050 Tomsk, Russia

To optimise the system, the results of numerical simulation were used at all stages. A numerical model for amplifying laser radiation in a XeF(C–A) amplifier of the THL-100 laser system was proposed in Refs [3, 4]. A good agreement is shown between the calculated and measured values of the energy and the spatial distributions of the energy density of the output radiation. However, the calculations did not take into account the spectral composition of the radiation at the entrance to the gas amplifier, i. e., the frequency-modulated laser radiation, the spectral composition of which is determined by the parameters of the radiation entering the stretcher. This radiation is transform limited and has a spectrum width of $\Delta\lambda \approx$ 7 nm and a pulse duration of 50 fs [7]. The stimulated emission cross section at the XeF(C–A) transition depends on the wavelength [8]. Therefore, the frequency modulation of the input laser radiation can cause noticeable changes in both the energy and the pulse duration of the output radiation.

This work was carried out as part of a series of studies aimed at increasing the power and energy of laser radiation from the hybrid THL-100 laser system. The aim of the work is to study the effect of frequency modulation of the input laser radiation with subnanosecond pulse duration on the energy and time characteristics of the output radiation of a high-power THL-100 laser system.

2. Numerical model and calculation method

To study the effect of frequency modulation on the gain characteristics, it is necessary to take into account the frequency–time distribution of the energy density of the input laser radiation. In the experiment, a frequency-modulated laser pulse is formed in a stretcher, at the input of which a pulse of transform-limited laser radiation with the duration τ_0 = 50 fs is applied. In the present work, the stretcher is modelled by a medium with group-velocity dispersion (silica) [9].

2.1. Frequency–time distribution of the input radiation energy density

The dependence of the complex amplitude of the field of a Gaussian pulse on the distance l travelled in a dispersive medium is well known [10]:

$$A(\eta, l) = V^{-1/2}(l)\rho_0 \exp\left\{-\frac{\eta^2}{2\tau_0^2 V^2(l)} + i\frac{(l/L_d)^2}{2V^2(l)k_2 l}\eta^2\right.$$
$$\left. -\frac{1}{2}\arctan\frac{k_2 l}{\tau_0^2}\right\}, \tag{1}$$

where

$$V(l) = [1 + (l/L_d)^2]^{1/2}; \quad \tau(l) = V(l)\tau_0; \tag{2}$$

τ_0 is the duration of the radiation pulse at a half-maximum level at $l = 0$; $\tau(l)$ is the pulse duration at a distance l; η is the time in the coordinate system travelling with the pulse; k_2 is the coefficient characterising the group velocity dispersion; and L_d is the dispersion length. At $\lambda = 475$ nm, the calculated value of k_2 for silica is 8.74878×10^{-26} s^2 m^{-1}, and the value of L_d [10] is 7.14 mm.

The distribution of the energy density of the laser radiation was calculated using the Wigner distribution function $W(\eta, \omega)$. This approach is used in time–frequency analysis of signals in nonlinear optics, tomography, etc. [11–15]. However, there are few studies on the frequency–time analysis of laser radiation with femtosecond and subnanosecond pulse durations, which is partly due to the difficulty of recording the Wigner distribution in this case. Nevertheless, such works are known. For example, the measured and calculated Wigner distributions coinciding with good accuracy are presented in Ref. [16], which, in our opinion, is an argument in favour of the correctness of the considered approach.

For pulses $A(\eta, l)$, the Wigner distribution has the form [11]

$$W(\eta, \omega, l) = \frac{1}{2\pi} \int_{-\infty}^{\infty} A^* \left(\eta - \frac{\zeta}{2}, l \right) A \left(\eta + \frac{\zeta}{2}, l \right) \exp(-i\omega\zeta)\, d\zeta, \quad (3)$$

where ζ is a parameter; ω_0 is the carrier frequency; and ω is the frequency. The total energy of the pulse is expressed as

$$E(l) = \frac{1}{2\sqrt{\mu_0/\varepsilon}} \int_{-\infty}^{\infty} d\eta \int_{-\infty}^{\infty} W(\eta, \omega, l)\, d\omega$$

$$= \int_{-\infty}^{\infty} I(\eta, l)\, d\eta = \int_{-\infty}^{\infty} S(\omega, l)\, d\omega. \quad (4)$$

The radiation intensity $I(\eta, l)$ and the quantity $S(\omega, l)$ are proportional to the frequency and time integrals of the Wigner function, respectively [17]:

$$I(\eta, l) = \frac{1}{2\sqrt{\mu_0/\varepsilon}} \int_{-\infty}^{\infty} W(\eta, \omega, l)\, d\omega, \quad (5)$$

$$S(\omega, l) = \frac{1}{2\sqrt{\mu_0/\varepsilon}} \int_{-\infty}^{\infty} W(\eta, \omega, l)\, d\eta. \quad (6)$$

According to the physical meaning, $S(\omega, l)$ is the radiation energy density per unit frequency. The integral in Eqn (3) for Gaussian pulses is calculated analytically [11]. Using the results of Ref. [11] for the pulse (1), we obtain the Wigner function in the form:

$$W(\eta, \omega, l) = \rho_0^2 \frac{\tau_0}{\sqrt{\pi}} \exp \left[-\gamma(l)\eta^2 - \frac{(\omega - \beta\eta - \omega_0)^2}{\gamma(l)} \right], \quad (7)$$

where

$$\gamma(l) = \frac{1}{V^2(l)\tau_0^2}; \quad \beta = V^{-2}(l)(k_2 l/\tau_0^4). \quad (8)$$

The correctness of Eqns (7) and (8) was controlled by numerical integration of Eqn (3), when l/L_d changed from zero to 10. For $l/L_d > 10$, numerical integration with the required accuracy requires excessive computational resources.

In the general case, the function $W(\eta, \omega, l)$ is always real-valued and can be both positive and negative, which complicates its interpretation as an energy density distribution [11].

However, for Gaussian pulses of form (1), (2), the Wigner function is always positive, which [taking into account Eqns (4)–(6)] allows it to be used to describe the time–frequency distribution of the energy density of a laser pulse entering the gas amplifier.

2.2. Gain calculation

The laser cell of the THL-100 gas amplifier is cylinder-shaped with a radius of 12 cm and an active region of 110 cm. The Ne–XeF$_2$ gas mixture is excited by VUV radiation with $\lambda = 172$ nm through windows located on the side surface of the laser cell. The active medium in the amplifier is formed by the interaction of VUV pump radiation with XeF$_2$ molecules, during the photolysis of which vibrationally excited XeF molecules (B,C) are formed. As a result, the VV and VT relaxation, the molecules are transferred to zero vibrational levels of the states XeF(B,C). Laser radiation is generated when XeF(C) molecules are transferred to the XeF(A) dissipation state [18, 19].

The gain was calculated in two stages. At the first stage, in the Cartesian coordinate system xy, the distributions of the absorbed pump energy, gain, and plasma particle concentrations in the cross section of the laser cell were calculated and stored in the memory with a time step of 1 ns. The spatial distribution of the energy absorbed in the cross section of the amplifier at a pump energy of 270 J is given in Ref. [3]. The amplified laser radiation passes through the active medium 33 times as a result of reflection from 32 mirrors with gradually increasing diameter installed on the inner flanges of the laser cell.

The amplification of laser radiation was simulated in the cylindrical coordinate system $\alpha r z$, where α and r are the azimuth angle and the distance from the longitudinal axis of the laser beam, respectively, and z is the distance travelled by the laser beam in the amplifier. The z axis runs from the centre of the input window ($z = 0$) to the centre of the first mirror, then to the centre of the second mirror, and so on to the centre of the exit window.

The laser beam was introduced into the amplifier with a time delay $t = t_{in}$ from the moment of amplifier pump beginning. The propagation time of the laser beam in the amplifier is $t_{amp} = t - t_{in}$, and the distance passed by it is $z = t_{amp}c$ (c is the speed of light in vacuum). As z increases, the beam radius increases in accordance with the specified divergence angle Ω. The spatial distribution of the photon flux density of the input laser beam F_{in} is symmetrical with respect to the angle α, and its dependence on r and η is described by the Gauss function:

$$F_{in}(\alpha, r, \eta) = F_{pic} \exp \left(-2 \frac{r^2}{R_0^2} \right) \exp \left(-\frac{\eta^2}{T_{fw}^2} 4\ln 2 \right). \quad (9)$$

Here T_{fw} is the duration of the input pulse; R_0 is the radius of the input laser beam at a level of $1/e^2$; and F_{pic} is the maximum photon flux density of laser radiation, determined from the normalisation condition (9) to the total number of photons $E_{in}/(\hbar\omega)$ at the amplifier input.

For each pass of the active region of the amplifier by the radiation, the spatial distributions of the concentration $n_C(x, y, t)$ of XeF(C) molecules in the amplifier were read at the time when the radiation enters the active region and at the time of its exit. Then, using the two-dimensional interpolation method [20], we calculated the unperturbed (in the absence of interaction of laser radiation with the active medium) distri-

bution $n_C(\alpha, r, t_{amp})$ in the cross section of the laser beam. The spatial distributions of the laser radiation flux density $F(\alpha, r, z, t_{amp})$ and the concentration $n_C(\alpha, r, z, t_{amp})$ were found by solving a system of equations

$$\left[\frac{\partial}{\partial z} + K + \frac{1}{c}\frac{\partial}{\partial t_{amp}} - n_C(\alpha, r, z, t_{amp})\sigma_{CA}(\lambda)\right]$$

$$\times F(\alpha, r, z, t_{amp}) = 0, \qquad (10)$$

$$\left[\frac{\partial}{\partial t_{amp}} + \sigma_{CA}(\lambda)F(\alpha, r, z, t_{amp})\right]n_C(\alpha, r, z, t_{amp}) = 0. \qquad (11)$$

Here, K is the coefficient of decrease in the photon flux density of laser radiation due to beam expansion [21]; and $\sigma_{CA}(\lambda)$ is the cross section for stimulated emission at the XeF(C–A) transition [8]. A more detailed description of the model is given in [3, 4].

The system of Eqns (10), (11) was solved using the Runge–Kutta method with a constant step $h_z = h_t c$ [22]. The step size was chosen such that the maximum change in the flux density of laser radiation F at the step h_z does not exceed 5% of its maximum value at the given moment. Otherwise, the value of h_z was decreased, and $n_C(\alpha, r, z, t_{amp})$ and $F(\alpha, r, z, t_{amp})$ were recalculated to the new grid. The accuracy of the calculations was controlled by the difference between the total number of photons of laser radiation per pulse and the total number of XeF(C) molecules, which passed into the XeF(A) state as a result of the stimulated emission. The error in these calculations did not exceed 1%.

The model was tested for various gas mixtures at a pump energy of $E_{VUV} = 220$ J [23, 24], 260 J [24] and 270 J [3]. In all cases, there was good agreement between the simulation results and experimental data for both the output energy and the distribution of the radiation energy density at the exit window.

3. Calculation results and discussion

3.1. Input pulse characteristics

The frequency-modulated pulse arriving at the input of the laser cell is formed when passing a 50 fs pulse with a transform limited pulse with an energy of 2 mJ of distance l in a medium with a group velocity dispersion. When moving in such an environment, its frequency–time characteristics change, which were determined from the Wigner distribution. The FWHM duration of the laser pulse is denoted by $\Delta t(l)$. The duration of a $\Delta\eta(\lambda, l)$ radiation pulse with a wavelength λ at a distance l will be understood as the width of the distribution $W(\eta, \lambda, l)$ over time η at half-height at $\lambda = $ const. Under the width of the spectrum $\Delta\lambda(\eta, l)$ at time η we mean the width of the distribution $W(\eta, \lambda, l)$ over λ at time $\eta = $ const. The wavelength λ, for which at time η the distribution $W(\eta, \lambda, l)$ has the maximum value, we denote by $\lambda_{max}(\eta)$.

The Wigner distribution for a transform limited radiation pulse with a duration of 50 fs with $\lambda = 475$ nm and $\rho_0 = 1$ V m^{-1}, input into the dispersive medium, has the maximum value $W(\eta = 0, \lambda_{max}, 0) = 0.6$ J m^{-2} with $\eta = 0$ and $\lambda_{max} = 475$ nm. At the boundaries of the phase space ($\lambda = 460–490$ nm and $\eta = \pm 90$ fs), the value of the Wigner function decreases to 1×10^{-5} J m^{-2}. The width of the spectrum is $\Delta\lambda(0,0) \approx 7$ nm, which coincides with the data of Ref. [7], $\lambda_{max}(\eta) = 475$ nm for any values of η.

In the course of propagation through the dispersing medium, the frequency modulation of laser radiation appears [10], and the range of variation of the Wigner distribution with time increases. Figure 1 shows the function $W(\eta, \lambda, l)$ for the laser beam at a distance of $l = 5L_d$ with positive chirp. It can be seen that the pulse duration $\Delta t(l)$ increased to 300 fs, while the duration of the radiation pulse with the wavelength λ ($\Delta\eta(\lambda, l)$) does not depend on l and remains equal to $\Delta\eta(\lambda, 0)$, which differs from the experimental data [7].

This difference can probably be explained in the framework of the method of spectrograms based on the windowed Fourier transform [11]. Both spectrograms and experimental results depend on the window sizes in time and frequency. In particular, the duration for specific values of λ is the greater, the smaller the window size in frequency, and vice versa. However, a strict explanation of this fact requires additional research.
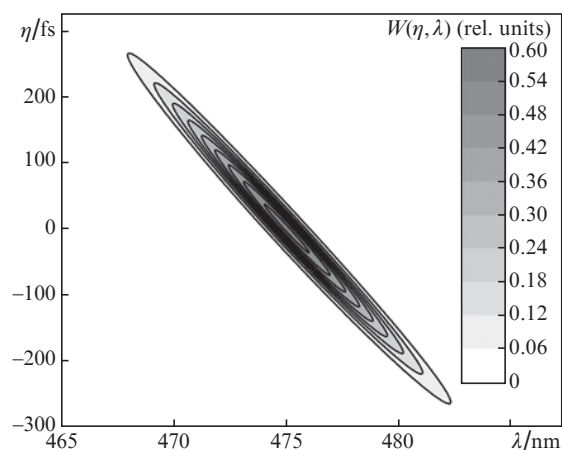

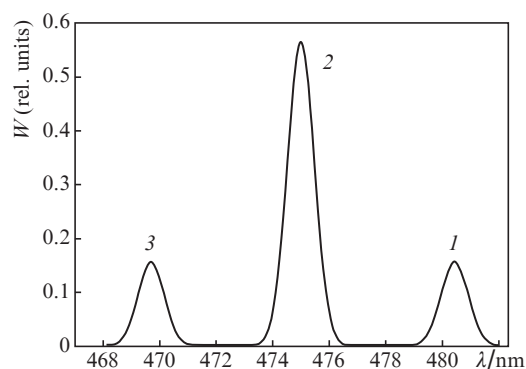**Figure 1.** Wigner distribution for a laser pulse transmitted through a distance of $l = 5L_d$ in a dispersive medium.

Figure 2. Cross sections of the Wigner distribution $W(\eta = $ const$, \lambda, l)$ with $l = 5L_d$ at time points $\eta = (1) -200$, (2) 0 and (3) 200 ps with positive chirp.

Frequency modulation of laser radiation is characterised by the appearance of a time dependence of $\lambda_{max}(\eta)$. Figure 2 shows the sections of the function $W(\eta, \lambda, l)$, shown in Fig. 1, in the plane $\eta = $ const at different points in time for positive chirp. With $\eta = -200$ ps, the maximum value of $W(\eta, \lambda, l)$ corresponds to radiation with $\lambda_{max}(\eta) = 469.5$ nm, and with $\eta = 200$ ps to the radiation with $\lambda_{max}(\eta) = 480.5$ nm.

With increasing l, the width of the spectrum $\Delta\lambda(0,l)$ decreases and reaches ~ 1.2 nm at a distance $l = 5L_d$. In general, the dependence $\Delta\lambda(0,l)$ can be obtained from the formula

$$\Delta\omega(0,l) = \sqrt{\gamma(l)\ln 2}, \qquad (12)$$

where the quantity $\gamma(l)$ is defined in Eqn (8). Figure 3 shows the change of $\Delta\lambda(0,l)$, calculated using Eqn (12), with increasing l/L_d from 0 to 5000. When $l/L_d < 1$, the width $\Delta\lambda(\eta,l)$ changes weakly and equals to ~ 6 nm. Then $\Delta\lambda(\eta,l)$ decreases to 1.3×10^{-3} nm for $l/L_d \approx 5000$. The value of $\lambda_{max}(\eta)$ linearly depends on time.
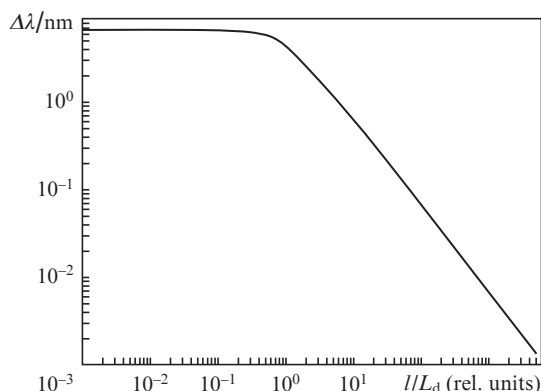

Figure 3. Width of the spectrum $\Delta\lambda(0,l)$ vs. the ratio l/L_d.

Thus, with an increase in the pulse duration, frequency modulation (chirping) of the radiation occurs. In the centre of the laser beam ($\eta = 0$) there are photons with a wavelength of $\lambda = 475$ nm. With a positive chirp at points $\eta = -250$ and 250 ps there are photons with wavelengths of $\lambda \approx 483$ and 467 nm, respectively. With a negative chirp, photons with a shorter wavelength are shifted to the beginning of the pulse. The results obtained allow us to conclude that to simulate the amplification of frequency-modulated radiation in this case one can use the system of Eqns (10), (11) for the photon flux density, assuming that at the time η the photons have a wavelength of $\lambda_{max}(\eta)$.

3.2. Gain characteristics

The gain of the input laser radiation was calculated for two cases. The input laser radiation was generated in a medium with normal group velocity dispersion (case A, positive chirp) and in a medium with anomalous dispersion (case B, negative chirp). The cross section of stimulated emission at each time instant η was determined by the value $\lambda_{max}(\eta)$ and the dependence of $\sigma_{CA}(\lambda_{max})$ on the wavelength [8].

With a positive chirp, the cross section $\sigma_{CA}(\eta)$ has a maximum value of 8.8×10^{-18} cm^2 with $\eta = -250$ ps and decreases to 7.2×10^{-18} cm^2 at $\eta = 250$ ps. In the case of a negative chirp, the cross section of the stimulated emission increases along the beam and reaches a maximum value of 8.8×10^{-18} cm^2 at the end point of the laser beam.

The simulation results showed that the frequency modulation of the input radiation under these conditions has little effect on the energy of the output radiation E_{out}. When the pump energy is $E_{VUV} = 270$ J, the laser energy is $E_{out} = 3.14$

and 3.11 J for cases A and B, respectively, which is because the amplifier operates in gain saturation mode. Frequency modulation has a more significant effect on the intensity and duration of the output laser pulse.

The maximum intensity $I_{max}(\eta)$ was calculated as the maximum value of the intensity of laser radiation in the section $\eta = $ const. At the pumping energy $E_{VUV} = 270$ J, the time dependences $I_{max}(\eta)$ for cases A and B are shown in Fig. 4. The results were obtained for the region of the 31st mirror (Fig. 1 from Ref. [3]), where the laser radiation intensity reaches maximum values of 1.2 and 0.8 GW cm^{-2}, respectively.
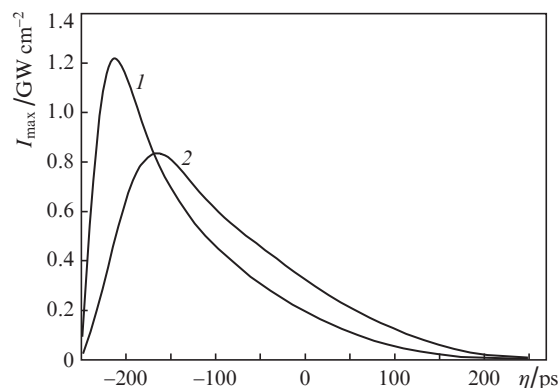

Figure 4. Maximum radiation intensity in the cross section of the laser beam as a function of time η for (_1_) positive and (_2_) negative chirps at $E_{VUV} = 270$ J.

The effect of the gain saturation effect leads to a shift of the maximum radiation intensity $I_{max}(\eta)$ from the point $\eta = 0$ to the region of negative values of η. With a positive input radiation chirp (case A), $I_{max}(\eta)$ reaches its maximum value when $\eta = -220$ ps. A decrease in the stimulated emission cross section in the central and final parts of the beam leads to an additional decrease in the radiation intensity in these regions. The output pulse duration Δt in this case is 102 ps.

With a negative input radiation chirp, the cross section $\sigma_{CA}(\eta)$ increases along the propagation direction of the laser beam and reaches a maximum in the final part of the beam. This partially compensates for the decrease in the concentration of XeF(C) molecules at the upper laser level in the region $\eta > 0$. The pulse duration of the output radiation in this case increases to 184 ps, and the maximum intensity value decreases from 1.2 GW cm^{-2} in case of A to 0.8 GW cm^{-2} in case B.

As the pump energy E_{VUV} increases to 400 J, the output radiation energy increases to 6.74 J with a negative chirp of the input radiation, which is already greater than the output energy (6.64 J) with a positive chirp. The calculated dependences of the pulse duration on E_{VUV} are shown in Fig. 5. In the entire range of variation of E_{VUV}, the output radiation pulse duration Δt_B for negative chirp is substantially longer than the duration Δt_A for positive chirp. With $E_{VUV} = 360$ J, the ratio $\Delta t_B/\Delta t_A$ reaches a maximum value of 3.75 and decreases to 3.2 when $E_{VUV} = 400$ J.

Figure 5 also shows the dependences of the maximum intensity of the output radiation in the amplifier I_{max} on E_{VUV} with positive and negative chirp of the input radiation. As E_{VUV} increases to 400 J, the intensity I_{max} increases to 10 and 4 GW cm^{-2}, respectively. Thus, the simulation results of the amplification of frequency-modulated radiation in the
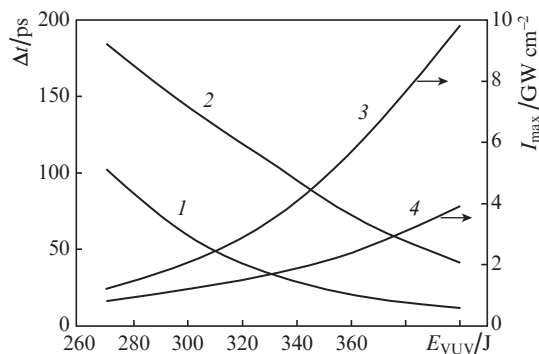
Figure 5. (*1, 2*) Pulse durations Δt of the output laser radiation at half-maximum level and (*3, 4*) maximum intensities I_{max} as functions of the pump energy E_{VUV} for (*1, 3*) positive and (*2, 4*) negative chirps of input radiation.

XeF(C–A) amplifier showed that the use of input radiation with a negative chirp can significantly increase the pulse duration of the output laser radiation and reduce its maximum intensity.

4. Conclusions

The influence of the frequency modulation of the input radiation on the gain characteristics of a 250-ps laser pulse in a gas XeF(C–A) amplifier of the THL-100 laser system at a pump energy of 270–400 J is investigated using numerical simulation methods.

The frequency–time distributions of the laser radiation energy density were calculated using the Wigner distribution function. Analysis of the results showed that in the case of pulse propagation in a medium with group velocity dispersion, as its duration increases from 50 fs to 250 ps, the width of the emission spectrum at the centre of the laser beam decreases from 7 to 1×10^{-3} nm.

The amplification characteristics of laser beams with positive and negative chirps are investigated. It has been found that in the gain saturation mode, the frequency modulation of the laser radiation at the input of the gas amplifier of the THL-100 facility has little effect on the output energy. At the pump energy $E_{VUV} = 270$ J, the laser energy E_{out} was 3.14 and 3.11 J with positive and negative chirp, respectively. Increasing E_{VUV} to 400 J leads to an increase in E_{out} to 6.64 and 6.74 J, respectively.

It was shown that the output radiation pulse duration Δt_B with a negative chirp is significantly longer than the pulse duration Δt_A with a positive chirp. With increasing pumping energy, the ratio of the duration of the output radiation pulse with negative and positive chirp $\Delta t_B/\Delta t_A$ increases and reaches a maximum value of 3.75 at $E_{VUV} = 360$ J. The maximum values of the laser intensity at $E_{VUV} = 400$ J are 10 and 4 GW cm^{-2} with positive and negative chirp, respectively.

References

1. Basov N.G., Zuev V.S., Mikheev L.D., Stavrovsky D.V., Yalova V.I. *Sov. J. Quantum Electron.*, **7**, 1401 (1977) [*Kvantovaya Elektron.*, **4**, 2453 (1977)].
2. Mikheev L.D. *Laser Part. Beams*, **10**, 473 (1992).
3. Yastremskii A.G., Ivanov N.G., Losev V.F. *Quantum Electron.*, **46**, 982 (2016) [*Kvantovaya Elektron.*, **46**, 982 (2016)].
4. Alekseev S.V., Aristov A.I., Grudtsyn Ya.V., Ivanov N.G., Kovalchuk B.M., Losev V.F., Mamaev S.B., Mesyats G.A., Mikheev L.D., Panchenko Yu.N., Polivin A.V., Stepanov S.G., Ratakhin N.A., Yalova V.I., Yastremskii A.G. *Quantum Electron.*, **43**, 190 (2013) [*Kvantovaya Elektron.*, **43**, 190 (2013)].
5. Alekseev S.V., Aristov A.I., Ivanov N.G., Kovalchuk B.M., Losev V.F., Mesyats G.A., Mikheev L.D., Panchenko Yu.N., Ratakhin N.A. *Laser Part. Beams*, **31**, 17 (2013).
6. Losev V.F., Alekseev S.V., Ivanov M.V., Ivanov N.G., Mesyats G.A., Mikheev L.D., Panchenko Yu.N., Ratakhin N.A., Yastremskii A.G. *Proc. SPIE*, **10254**, 1025415 (2017).
7. Alekseev S.V., Ivanov N.G., Ivanov M.V., Losev V.F., Mesyats G.A., Mikheev L.D., Panchenko Yu.N., Ratakhin N.A., Yastremskii A.G. *Quantum Electron.*, **47**, 184 (2017) [*Kvantovaya Elektron.*, **47**, 184 (2017)].
8. Bischel W.K., Eckstrom D.J., Walcker H.C. Jr., Tilton R.A. *J. Appl. Phys.*, **52**, 7 (1981).
9. http://glassbank.ifmo.ru/rus/prop.php?id=449#.
10. Akhmanov S.A., Vysloukh V.A., Chirkin A.S. *Optics of Femtosecond Laser Pulses* (New York: AIP, 1992).
11. Cohen L. *Time-Frequency Analysis* (Upper Saddle River, New Jersey: Prentice-Hall PTR, 1995).
12. Rulliere C. *Femtosecond Laser Pulses. Principles and Experiments* (New York: Springer, 2003).
13. Dragoman D. *Appl. Opt.*, **35**, 21 (1996).
14. Belabas N., Likforman J., Conioni L., Bouscuet B., Joffre M. *J. Opt. Soc. Am.*, **69**, 12 (1979).
15. Praxmeyer L., Wódkiewicz K. *Laser Phys.*, **15**, 10 (2005).
16. Belabas N., Likforman J., Conioni L., Bousquet B., Joffre M. *Opt. Lett.*, **26**, 10 (2001).
17. Diels J.C., Rudolph W. *Ultrashort Laser Pulse Phenomena. Fundamentals, Techniques, and Applications on a Femtosecond Time Scale* (San Diego, California: Academic Press, 2006).
18. Malinovsky G.Ya., Mamaev S.B., Mikheev L.D., Moskalev T.Yu., Sentis M.L., Cheremiskin V.I., Yalovoy V.I. *Quantum Electron.*, **31**, 617 (2001) [*Kvantovaya Elektron.*, **31**, 617 (2001)].
19. Ivanov N.G., Losev V.F., Panchenko Yu.N., Yastremskii A.G. *Atmos. Oceanic Opt.*, **27** (4), 329 (2014) [*Opt. Atmos. Okeana*, **27** (4), 326 (2014)].
20. Fletcher C.A. *Computational Techniques for Fluid Dynamics* (Berlin-Heidelberg: Springer-Verlag, 1988; Moscow: Mir, 1991).
21. Kuznetsova T.I., Mikheev L.D. *Quantum Electron.*, **38**, 969 (2008) [*Kvantovaya Elektron.*, **38**, 969 (2008)].
22. Fleck J.A. Jr. *Phys. Rev. B*, **1**, 84 (1970).
23. Alekseev S.V., Ivanov N.G., Losev V.F., Panchenko Yu.N., Yastremskii A.G. *Opt. Atmos. Okeana*, **26**, 863 (2013).
24. Losev V., Alekseev S., Ivanov N., Kovalchuk B., Mikheev L., Mesyats G., Panchenko Yu., Puchikin A., Ratakhin N., Yastremsky A. *Proc. SPIE*, **7993**, 799317 (2011).